Horizon 2020

Project acronym: **LASH FIRE**

Project full title: **Legislative Assessment for Safety Hazard of Fire and Innovations in Ro-ro ship Environment**

Grant Agreement No: **814975**

Coordinator: **RISE Research Institutes of Sweden**

Deliverable D08.10

Demonstration of prototype for detection of potential ignition sources

August 2023

Dissemination level: **Public**

Abstract

To improve fire safety in ro-ro spaces on ro-ro ships, usage of remote sensing and robotics addresses at least three challenges for humans: presence at risk locations, presence over time, and reaching difficult locations. There is no single solution that can passively and unintrusive, monitor and detect all ignition sources. A system of systems approach would be needed, as well as close interaction and assistance for human operators to achieve an enhanced situational awareness. This task can be addressed with stationary or moving systems. Each has benefits and drawbacks. Stationary systems need to be located relatively near and with free line of sight to the object. A mobile system can position itself to achieve good presence, but the sensor array and endurance will be limited. The systems should not be intrusive/physical since it will have huge impact on the flow of units or the risk of damage to the object. Both the stationary Vehicle Hotspot Detection (VHD) and Automatic Guided Vehicle (AGV) -systems are on based existing products and modified for a LASH FIRE purpose.

The platforms were modified with additional sensors and corresponding development of software and algorithms to perform the needed tasks. The VHD and AGV systems was tested and verified during 2022 and demonstrated in late 2022 early 2023, results are presented in: D08.11 "Description of prototypes and demonstration for identification of vehicles and ignition sources".

This project has received funding from the European Union's Horizon 2020 research and innovation programme under grant agreement No 814975

Document data

Document Title:	D08.10 - Demonstration of prototype for detection of potential ignition sources		
Work Package:	WP08 – Ignition		
Related Task(s):	T08.8		
Dissemination level:	Public		
Deliverable type:	DEM, Demonstration		
Lead beneficiary:	1 – RISE		
Responsible author:	Martin Torstensson		
Co-authors:	Robert Rylander, Leon Sütfeld		
Date of delivery:	2023-08-14		
References:	D08.1, D08.9		
Approved by	Francisco Rodero CIM on 2023-08-14	Erik Styhr Petersen NTNU on 2023-08-14	Maria Hjohlman RISE on 2023-08-14

Involved partners

No.	Short name	Full name of Partner	Name and contact info of persons involved
01	RISE	RISE Research Institutes of Sweden AB	Martin Torstensson, martin.torstensson@ri.se
13	SCK	SICK AG	Markus Haas, markus1.haas@sick.de

Document history

Version	Date	Prepared by	Description
01	2021-10-01	Martin Torstensson	Draft of structure
02	2023-03-17	Martin Torstensson	Draft of final report
02	2023-03-28	Martin Torstensson	Draft sent for review
03	2023-06-15	Martin Torstensson	Second draft of final report
04	2023-08-14	Robert Rylander	Final draft for review

Content

1 Executive summary

Usage of remote sensing and robotics addresses at least three challenges for humans, presence at risk locations, presence over time, and reaching difficult locations. Currently, there is no single solution that can passively and unintrusive monitor and detect all ignition sources. A system of systems approach would be needed and close interaction and assisting human operators, which could enhance situational awareness. This task can be addressed with stationary or moving systems, they have benefits and drawbacks. Stationary systems need to be located near and with a free line of sight to the object. Moving system can position them self to achieve good presence but the sensor array and endurance will be limited. The systems should not be intrusive/physical since it will have huge impact on the flow of units or the risk of damage to the object.

Governments are concerned with the introduction of Alternative Powered Vehicles (APV) and the more complex situation they produce onboard the cargo deck. UK Maritime Coastguard Agency (MCA) issued a Guidance document MGN 653 (M) Electric vehicles onboard passenger roll-on/roll-off (ro-ro) ferries [1] which emphasizes the need for more knowledge about the vehicles from booking all the way to storage onboard the ship, also suggesting extra marking, tracking, and positioning of APVs on the ship.

1.1 Problem definition

Fire prevention on ships is a challenge that stretches across different locations and times. Once the cargo is loaded onto the ship, extinguishing fires or removing the cargo are more difficult, especially in the case of electric vehicles when thermal runaway has taken place. It is, therefore, of importance to reduce the potential fire hazards at an early stage, preferably preventing a fire by re-directing cargo with high risk before loading. On the other end of the spectrum some hazards are not present until the voyage has already started and cannot be identified on shore. Continuous monitoring is needed to efficiently find potential ignition sources before a fire erupts, allowing for appropriate safety measures to be taken.

1.2 Technical approach

One system would not be enough to cover both the needs of monitoring the cargo before loading and during the voyage. Instead, a two-system approach has been applied where a Vehicle Hotspot Detection (VHD) system is active on shore and an Automatic Guided Vehicle (AGV) offshore. The VHD acts as a gate, which the cargo transport passes through. With the aid of thermal cameras, it scans the objects passing through and detects if there are heat anomalies and where they are located. Based on this information it is possible to stop cargo from boarding, removing it for further inspection. The AGV is located inside of the ship's cargo space and is activated once the loading is finished. It can then continuously navigate around the cargo space and scan cargo and vehicles from underneath for abnormal heat signatures with a thermal camera.

While this report focuses on the demonstrator and tests of the ignition source detection more background of the challenges and reasoning behind the approach can be found in D08.2 - Fire hazard mapping visualization tool with fire hazard matching integrated [2]. Moreover, the design choices and components of the systems can be found in D08.11 - Description of prototypes and demonstration for identification of vehicles and ignition sources [3].

1.3 Results and achievements

Two demonstrators have been created, one for the VHD system and one for the AGV.

Among the conclusions that could be made from the tests performed with the AGV are:

- Thermal imaging from underneath vehicles is possible with an AGV.
- The choice of LiDAR is crucial for navigation involving moving underneath objects.

From the demonstrator of the VHD system the following results were extracted:

- Adding a second LiDAR used for measurements and tracking of the vehicle, mitigated the challenges and limitations a limited space available at the Majnabbe terminal.
- The second LiDARs precise measurements and tracking of the vehicles made it possible to successfully segment out the refrigeration units with the help of machine learning.
- The third LWIR sensor facing downwards could get a free line of sight of the top of the refrigeration units.
- The added hardware and development of the TEMS software have successfully raised alarms to the operator of the VHD at the desired temperature threshold.

The modifications made to the VHD system have worked as intended. A terminal, ship or freight operator can gain knowledge about the incoming cargo/vehicles with the use of a remote sensing system. The system can detect heat signature from various parts of the object and with a LASH FIRE configuration even the refrigeration unit with minor or no impact of the flow of the vehicles. This raises the situational awareness from random to a systematic approach, and depending on the operation, the threshold levels for an alarm can be configured to match their operation. Late arrivals can be monitored in real time as they pass through the sensor arch and if they show signs of overheating, actions can be taken directly before they are allowed onboard. They could be stowed on the weather deck if possible or stopped from being loaded at all.

1.4 Contribution to LASH FIRE objectives

The deliverable is directly tied to T08.8, where a demonstrator for detection of potential ignition sources is to be presented and is part of the automatic screening solution in the objectives of WP8. The report covers the demonstrator and the tests performed. More information on design choices and construction of the AGV can be found in D08.11 - Description of prototypes and demonstration for identification of vehicles and ignition sources. Additionally, the background for the development and the challenges that have been taken into consideration can be found in D08.2 - Fire hazard mapping visualization tool with fire hazard matching integrated.

1.5 Exploitation and implementation

This report serves as a demonstration report and more information on details and exploitation can be found in D08.11 - Description of prototypes and demonstration for identification of vehicles and ignition sources.

2 List of symbols and abbreviations

2D	Two Dimensional
3D	Three Dimensional
AC	Automatic Climate control unit
ADR	A Accord européen relatif au transport international des marchandises Dangereuses par Route
AFV	Alternative Fuel Vehicle, see APV
AGV	Automated Guided Vehicle
APU	Application Programmable Unit
APV	Alternative Powered Vehicle, this includes battery, hybrid, gas and future sources of power to propel a vehicle.
FOV	Field of view
FRMC	Firefighting Resource Management Centre
HW	Hardware
IMDG	International Maritime Dangerous Goods Code
LiDAR	Light Detection and Ranging sensor
LWIR	Longwave Infrared
ML	Machine Learning
Reefer	Refrigeration Unit e.g. air conditioning unit on a trailer or container
RoRo	Roll On- Roll Off general cargo ships
RoPax	Roll On -Roll Off Passenger ships
SLAM	Simultaneous Localization And Mapping
SPT	Stowage Planning Tool
SW	Software
VDG	Vehicle Dangerous Goods detection system
VHD	Vehicle Hotspot Detection system

3 Introduction

Based on historical data and previous projects; FIRESAFE 1& 2 [4], Lighthouse In-door positioning on RoRo vessels [5], these studies include conclusions taken from the fire cause perspective and highlights the differences in fire sources, from the ship's equipment and the cargo. The statistics regarding the probability related to fires originating in ro-ro spaces was performed and subsequently used as input for a Hazard Identification (HAZID) workshop [6] where the main takeaways are:

- The ship's equipment is rarely the cause of fire, rather the ship's cargo is generally the culprit.
- Electrical fault originating in the ship's cargo is the most common cause of fires in ro-ro spaces.
- Although refrigerated units typically constitute a relatively limited proportion of all the carried cargo onboard it is statistically the most fire hazardous type of cargo in terms of probability and severity.
- While electrical failures in internal combustion engine vehicles constitute an apparent hazard, especially if the vehicles are in poor condition, there is little, if any, data that suggests electrical vehicles are more prone to fire than internal combustion engine vehicles.
- Gas leaks in Alternatively Powered Vehicles (APV) that leads to fire is a rare occurrence.

Based on this, automatic remote sensing systems are investigated as a tool to support the personnel and crew at the different phases, terminal, loading and during the voyage.

A fixed system based on VHD and a ground system based on AGVs were modified for LASH FIRE. The primary goal is systems that can detect heat anomalies, and quantitative measurements for continuous observation of objects.

This is a step towards a system of systems approach where different systems communicate and collaborate with the personnel and crew to provide quantitative measurements and better situational awareness.

4 VHD vehicle identification prototype

Main author of the chapter: Robert Rylander, RISE

4.1 General description of prototype

The VHD is a sophisticated non-intrusive remote sensing system originally used to increase road safety at some of the longest or most critical road and rail tunnels in Europe, for example, it is used in the Gotthard road tunnel. As objects pass through a gantry, where a suite of sensors is placed, data is collected and used in the Traffic Enhanced Monitoring software (TEMS) to compute and fuse the data with images into a user-friendly interface, which provides an operator with a read out of all the sensor data. Both two- and three-dimensional visualization is available.

In the LASHFIRE project the VHD system is equipped with color and monochrome cameras, extra Longwave Infrared (LWIR) cameras and digital ambient temperature sensors and an extra Light Detection and Ranging (LiDAR) unit. The concept is illustrated below.

Figure 1 Illustration of the concept of the LASHFIRE VHD sensor portal (SICK)

In the illustration below is the VHD systems new innovative concept with two LiDARs illustrated.

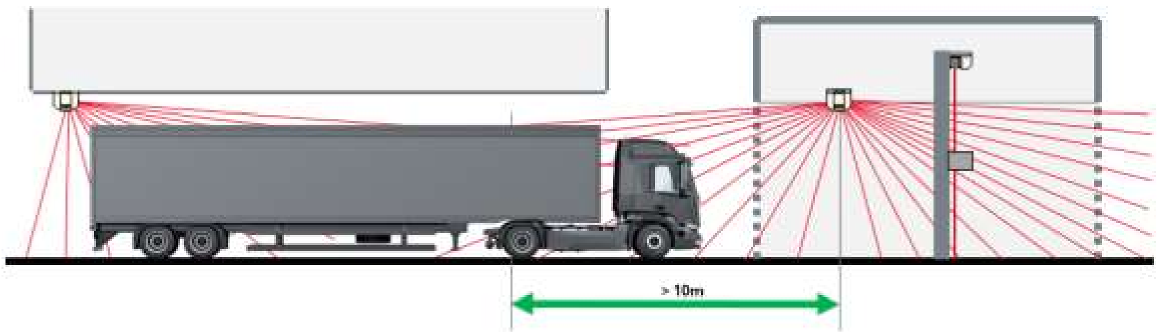

Figure 2 The extra LiDAR is placed at left and the original to the right. (SICK)

4.1.1 Test design

The test campaign was set up as two phases, the first phase to set up and validate the LASHFIRE modifications to the VHD system. This included hardware and software modifications and

developments.
Extra hardware installations of the demonstrator:
- A third LWIR sensor, facing downwards to the topside of the vehicle to capture the heat signature of the top of the refrigeration unit.
- Extra license plate reader for the trailers.
- An additional LiDAR for accurate length, width, and height measurements to support the segmentation of the vehicle's different parts.

Software development for the third LWIR sensor and LIDAR and training of the machine learning (ML) algorithm that is one method used to segment out the refrigeration units on the trucks and trailers.

To support the modifications and development of the VHD, quantitative data was collected on the refrigeration trucks and trailers that passed the VHD system was conducted and feed both as data sets for training of the ML and to determine a normal temperature range for refrigeration units running on their combustion engines as the passed the VHD system.

The second phase was a demonstration including for the Stena Line personnel at Majnabbe terminal and a test on how a VHD system could be implemented into the procedures at the terminal and the ship that is to be loaded.

Based on the demonstration these requirements and LASH FIRE functions needed to be implemented and tested

Table 1 New requirements on the VHD system.

R#	Functional element	Requirement	Test
VL.1	Positioning & profiling, LiDAR	Capture front and rear of vehicle entering the gate using forward LiDAR	VLT 1a
VL1.1	Positioning & profiling, LiDAR	Capture front and rear of vehicle entering the gate using rear LiDAR	VLT 1b
VL.2	Positioning & profiling, LiDAR	Track vehicle as is moves through the gate	VLT2
VL3	Positioning & profiling, LiDAR	Length measurements of vehicle, precision less than 0,4m	VLT3
VL.4	Positioning & profiling, LiDAR	Profiling of the sides of vehicle	VLT4
VL.5	Positioning & profiling, LiDAR	Profiling of the top side of vehicle	VLT5
VT.1	Thermographic profiling, LWIR	LWIR captures the sides of the vehicle	VTT1
VT.2	Thermographic profiling, LWIR	LWIR captures the top side of the vehicle	VTT2

LASH FIRE functions needed to be developed in the TEMS software.

Table 2 New functionality in the VHD system.

F#	Functional element	Requirement	Test
VS.1	TEMS SW development	Incorporate length measurement using two LIDARs	VST.1

VS.2	TEMS SW development	Incorporate downward profiling LIDARs	VST.2
VS.3	TEMS SW development	Incorporate downward thermographic LWIR	VST.3
VS.4	TEMS SW development	Use machine learning algorithm to detect refrigeration unit on trailers	VST.4
VC.1	Clients	Allow presentation of new sensors	VCT. 1

4.1.2 Scenario description

Every day on the year, refrigeration units are shipped on RoRo/RoPax-ships, and they arrive at the terminals around the clock, if loaded they are usually running on internal combustion engines. The LASH FIRE demonstration needed a route with a flow of refrigeration units that was actively running and not empty and shut off. To achieve the goal that automatically screen for refrigeration units, segment the refrigeration automatic climate control (AC)-unit out on the truck and/or trailer and then raise an alarm if a temperature anomaly is detected.
To do this, collecting temperature readings from the refrigeration units has to be done and a analysis performed on the data set to find a base line for a temperature range of normal operation. This is a manual operation to screen for refrigeration units and at the same time collect refrigeration units to build training and validation sets for the machine learning algorithm.

When the VHD systems machine learning algorithm supported detection of refrigeration units it was manually validated and then used in the demonstration for the rest of the tests.

The usability demonstration of the LASHFIRE VHD LFVHD was divided in to three stages as descried below.

Table 3 VHD practical test phases and criteria.

	First test week (testing alarm function)	Test month (testing complete procedure)	Full operation (fire prevention)
Temperature criteria for alarm*	85	110	150
Expected number of alarms	10/week	3/week	1/month
Action on alarm	No action	Manual inspection	Manual inspection, Masters decision

* Temperature criteria was bases on the collected data set May to October 2022.

Segmentation of parts of the vehicle

Segmentation of the vehicle is done in the TEMS software, there are two functions working in parallel. One is depending on a technician at SICK to create areas of interest and they are then matched onto the thermographic images illustrated below.

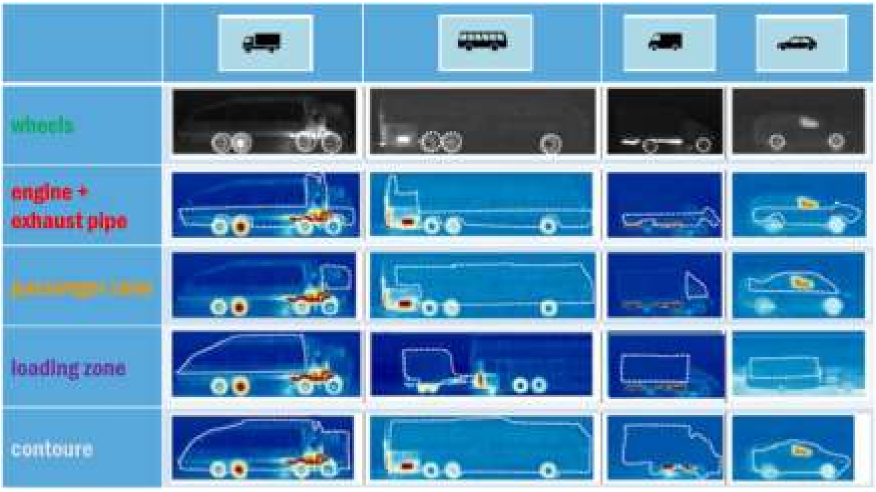

Figure 3 Segmentation based on predefined areas of interest. (SICK)

For each segment and type of vehicle, different temperature thresholds for raising an alarm level can be set.

The second way is the usage of machine learning algorithms and a neural network. The algorithm is trained on one set of data then tested on a different set and then if it performs well, it can be incorporated into the live software that runs at the designated VHD system.

4.2 VHD demonstration site

The planning for the Demo started in November 2019, and during the winter and spring 2020, the first proposed location was an installation at Stena Line terminal in Karlskrona, Sweden. In Karlskrona Stena Line had a test site for new gate and booking technologies for a future automated check in procedures.

4.2.1 Demonstration site shifted from Karlskrona to Majnabbe

Preparation was made for an installation illustrated below underneath a roof and the horizontal and vertical steel beams was the main point for mounting the sensor array.

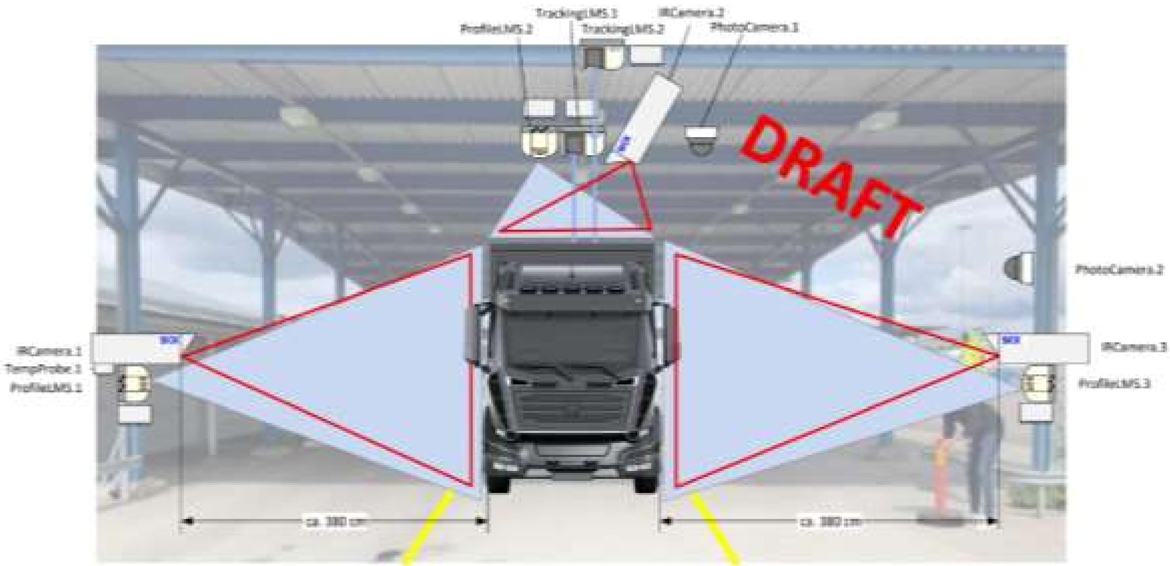

Figure 4 Planned installation at Karlskrona looking from the front.

And from above it would look as illustrated below:

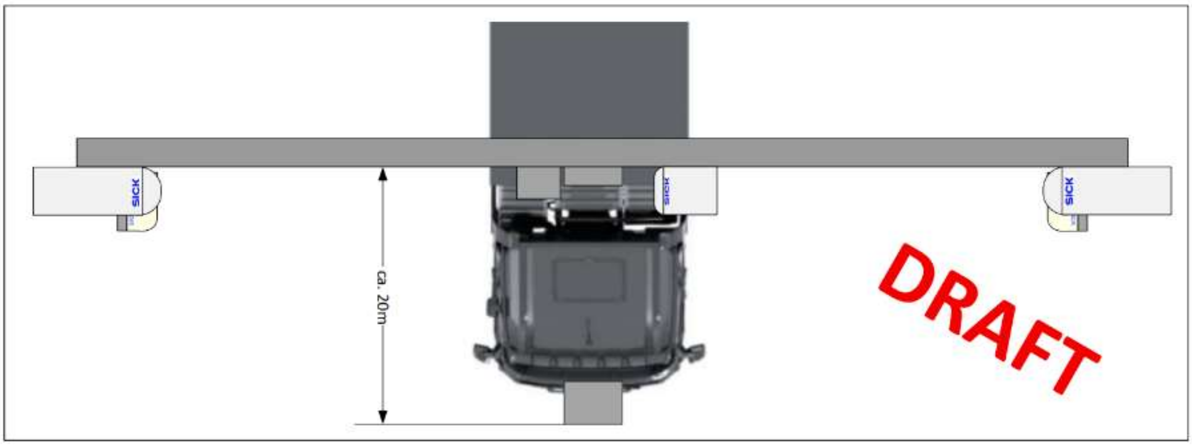

Figure 5 Vertical view of sensor array at Karlskrona.

During meetings held in June and July 2020 the decision was made to make new plans for installation at the Stena Line terminal at Majnabbe in Gothenburg. Majnabbe has a better flow of refrigeration units but a smaller location to install the sensors at. The flow of refrigeration units is important.

4.2.2 Majnabbe

In September 2020, the final on-site measurement was taken for the installation at Majnabbe. It was conducted with personnel from SICK, Stena Line and RISE. The design for the site-specific fastenings for the sensor installations could start and short after the fastenings and other hardware was ordered and manufactured. Illustrated below is the as is situation at Majnabbe.

Entrance for heavy vehicles to the Majnabbe terminal.
In the picture is the gate house (grey) and the raisable barrier is visual behind Jan Engquist from SICK.

Figure 6 Final planning and measurements taken on the building at Majnabbe, looking north.

Prior to the actual gate, there is an office building, and the lower floor windows are visible to the left in the picture above, and the first floors cement structure of the office building is barely visible at the top of the picture above. The front of the first floor is shown in the picture below.

Figure 7 Front edge of office building in front of the gate to the south.

The low vertical clearance of 490cm, obscures the line of sight for the traditional placement of the length and position measuring LiDAR.
It was decided to develop a new array and sensor layout with two LiDARs for length and positioning to be able to track the front and rear of the vehicle as illustrated in Figure 2 The extra LiDAR is placed at left and the original to the right. (SICK) with two downward facing LiDARs.

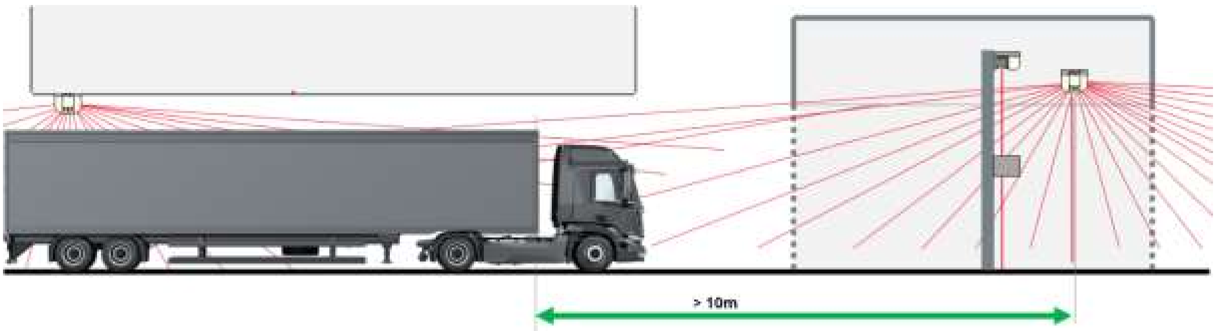

Figure 8 Illustration of the two LiDARs used in tandem for positioning and tracking. (SICK)

The new concept would look like illustrated below, with the two downward facing LiDARs on three sides for profiling the vehicle for the 3D model.

4.2.3 The Gatehouse

Figure 9 Left side of the gate house, looking south. (RISE)

Inside the gatehouse, Stena Line have a system for documenting all vehicles that passes the gate. The VHD system had to be adapted to the situation with the present system and its gantry portal arrangement. Our system did not interfere with its functions and our system still get a free line of sight. The LASH FIRE project benefitted from the present systems light arrangement.

4.2.4 LiDARs for length measurement and tracking

The systems use SICK LiDAR with lens flare protection as illustrated below.

Figure 10 LiDAR with flare protection and junction box. (SICK)

The installation has two types of LiDARs, three LMS511 with 180° lens opening for the top down mounted and LMS511 with 125° opening for side profiling of the vehicles.

Forward LiDAR for length and position measurements

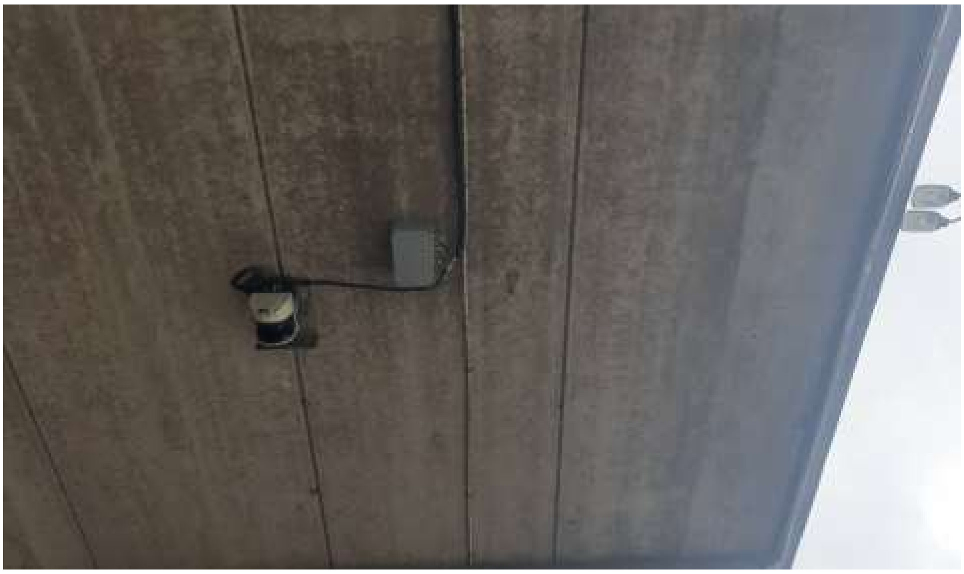

Figure 11 The forward LiDAR underneath the office building.

To create as long as possible stretch for the system to capture the forward and rear edge of a long truck and trailer, the forward LiDAR was placed close to the south edge of the office building.

Rear LiDAR for length and position measurements

As illustrated below, the aft LiDAR was placed low to get a longer free line of sight towards the entrance, it later showed that this was not enough, and a gap had to be opened at the rear of the gate house.

Figure 12 Second LiDAR plus forward license plate readers at the exit of the gate house.

4.2.5 LWIRs for thermographic heat mapping.

The system uses the same type of LWIR sensor and weather protection as illustrated below for all three positions top-down and right and left sides.

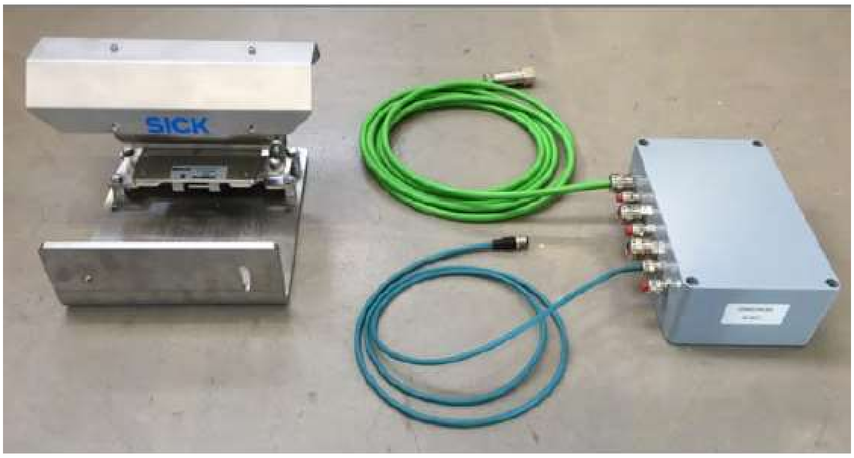

Figure 13 LWIR with bracket and junction box. (SICK)

In the picture below the LWIR is to the right of the LiDAR, both are in the centre of the picture.

Figure 14 Vertical installed LWIR and LiDAR (RISE)

LiDAR and LWIR sensors aligned.

Also visible in the upper part of the photo is present other systems installed cameras.

4.2.6 Side sensors

Right side vertical sensors

From the top:

CCTV color camera.

LWIR thermographic sensor.

LiDAR vertical profiling of the side of the vehicle.

Figure 15 Sensor for profiling and IR scanning the sides. (RISE)

Left side sensors.

The left side has the same set up as the right side, the only difference is the ambient temperature sensor visible as a small white box to the right of the vertical pillar in the image below.

Figure 16 Ambient temperature, LWIR and LiDAR. (STL)

Below is a view of the left side installations viewed from right side CCTV, the far-right grey cabinet is the VHD systems cabinet.

Figure 17 Left side viewed through the right sides CCTV.

VHD Cabinet

Figure 18 VHD system cabinet. (STL)

The main component in the cabinet is the Application Programmable Unit (APU) that runs the TEMS software. The cabinet also serve as power distribution to the sensors and the APU has an uplink with Internet connectivity.

Figure 19 Interior of an VHD Cabinet. (SICK)

The cables for power and signals are routed through the bottom of the cabinet.

Alarm indications

Figure 20 VHD status indications. (STL)

VHD system status can be viewed on the outside of the cabinet or via the TEMS software.

4.2.7 Incident with forward LiDAR

In October 2021, something high hit the forward LiDARs junction box, probably a truck and trailer that were too high. Luckily the installed safety bracket took all the damage and junction box and LiDAR received no damage.

Figure 21 Damage to junction box at Majnabbe. (STL

4.2.8 Challenges

Due to the low vertical clearance, the length measurements with two LiDARs were not accurate enough so an opening in at the exit from the gate house was done in December 2022. This allowed the rear LiDAR to track the exiting vehicle longer and there by achieving better accuracy of length and positioning of the vehicle.

Figure 23 Exit of gate house after modification. (STL)

The raisable barrier red and white fence in the center of the picture above, encircled in red in the image from the TEMS Analyzer software below. The barrier occasionally interfered with the length measurement and positioning of the vehicles as it moved into the gate house. The software was tweaked to ignore the barrier as much as possible.

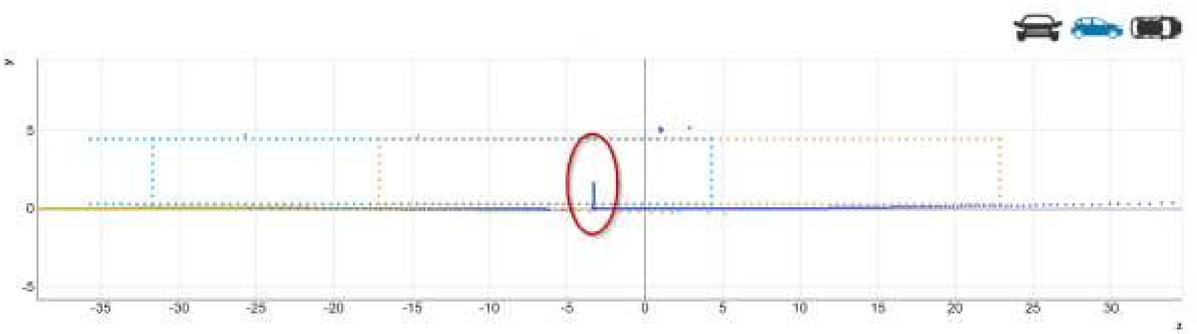

Figure 24 The blue "spike" inside the red circle is the raisable barrier seen in the TEMS Analyser.

4.2.9 VHD Client at Check-in

A laptop with VHD Client was placed at the Check-in at a counter, the staff was introduced to the client and kept a paper log of alarms.

	Date & Time	Note (Reg.Nr/Booking/Temperature/…)	FALSE
1			
2			
3			
4			
5			
6			
7			
8			
9			
10			

First unit that triggered an alarm

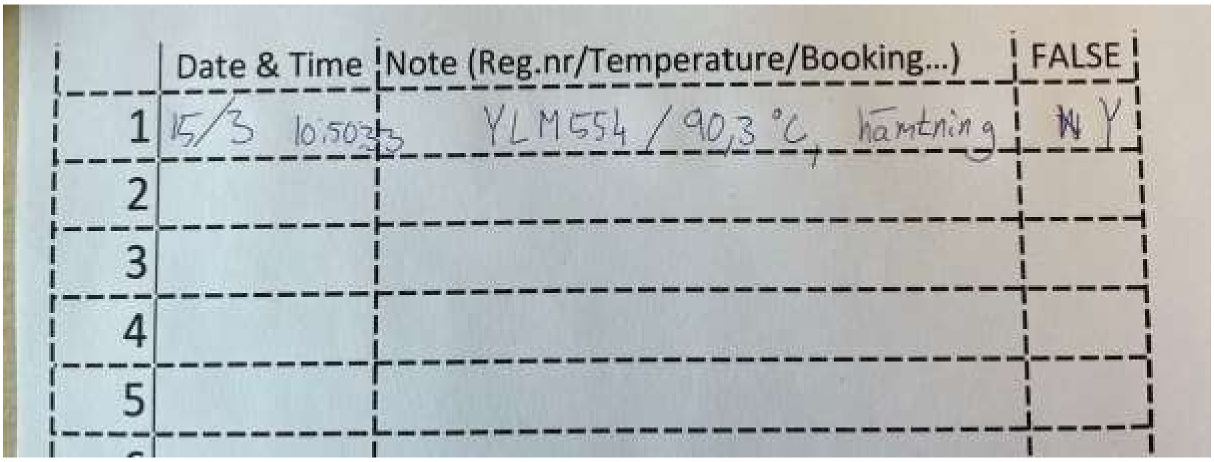

	Date & Time	Note (Reg.nr/Temperature/Booking…)	FALSE
1	15/3 10:50:33	YLM554 / 90,3 °C, hamtning	~~N~~ Y
2			
3			
4			
5			

Figure 25 Manual log entry from Majnabbe. (STL)

This entry in the log was a truck with high temperatures on another part of the truck, the alarm was not from a refrigeration AC unit and therefore logged as False in the perspective the the focus testing was on just refrigeration units. The VHD system was active for heat detection on all parts of the vehicle. During the demonstration the alarm levels temperatures were set to a temperature higher than normal for the other segments of the truck to have as relevant alarms as possible to start with. Later the temperatures were lowered, and more alarms could occur.

All data from the VHD system was also stored on an FTP server and kept as a record.

4.3 When a VHD alarm is raised

Reacting on an alarm has been discussed in different forums at Stena Line with personnel from Check-in, stevedores, ship and management.
How to perform an inspection when an elevated risk has been detected. Safety of the personnel, driver and passengers is the uttermost important and there are many factors to consider.

In general:

- How to protect the personnel when doing an inspection?
- How to protect other person in the vicinity?

- How to protect other vehicles? Any ADR/DG at the quay?
- How to protect infrastructure at the terminal?

- How to safely do the inspection?
  - Handheld Thermal camera?
  - Ladder access to topside of vehicle?
- How can we train the personnel that will do the inspections?

Then, how to decide if the unit is fit for shipping?

An alarm triggers the shore organization, below are three general steps that has been iterated during the demonstration. Depending on where the alarm is received and the terminals infrastructure, the response will be different.

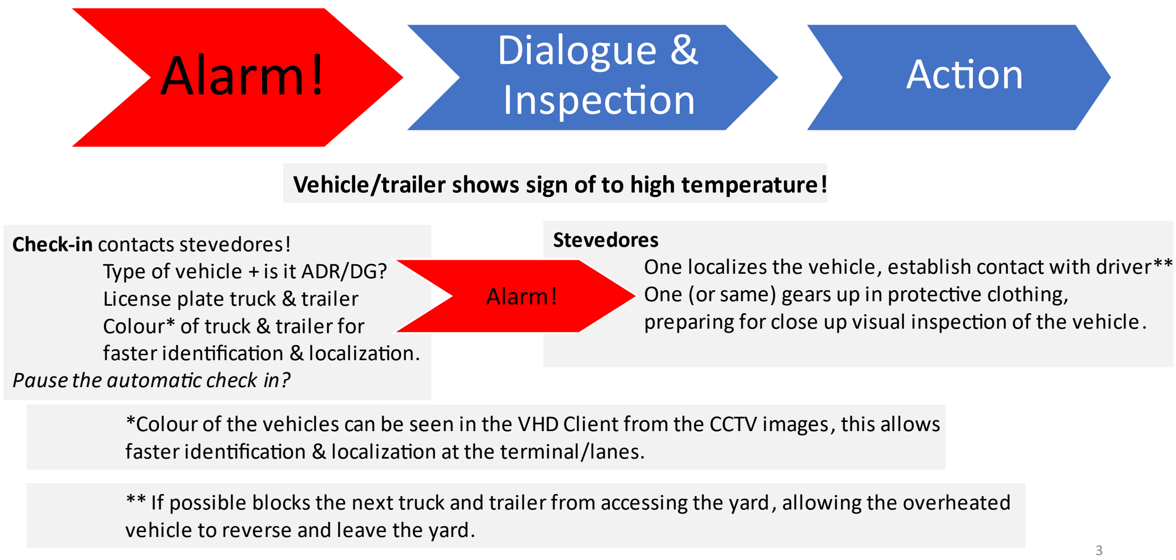

Figure 26 VHD Alarm is triggered.

The VHD user contact the support organization, at Majnabbe, this is the personnel at the quay that handles the loading operation. Information about the vehicle is communicated and the first goal is to locate the vehicle to start a dialogue with the driver and a first remote assessment of the vehicle. As fast as possible a decision on further actions has the be taken.

Figure 27 Dialogue with driver and is an Inspection possible to perform?

In the dialogue with the driver, he/she is informed about the situation and information about the vehicle(s) is obtained. The time for action can be short or very long depending on many factors, not only the temperature that has been recorded. Factors like: Is it an ADR/DG goods, can it easily be parked at a safer spot inside the terminal for further investigations and service or should it be sent outside directly?

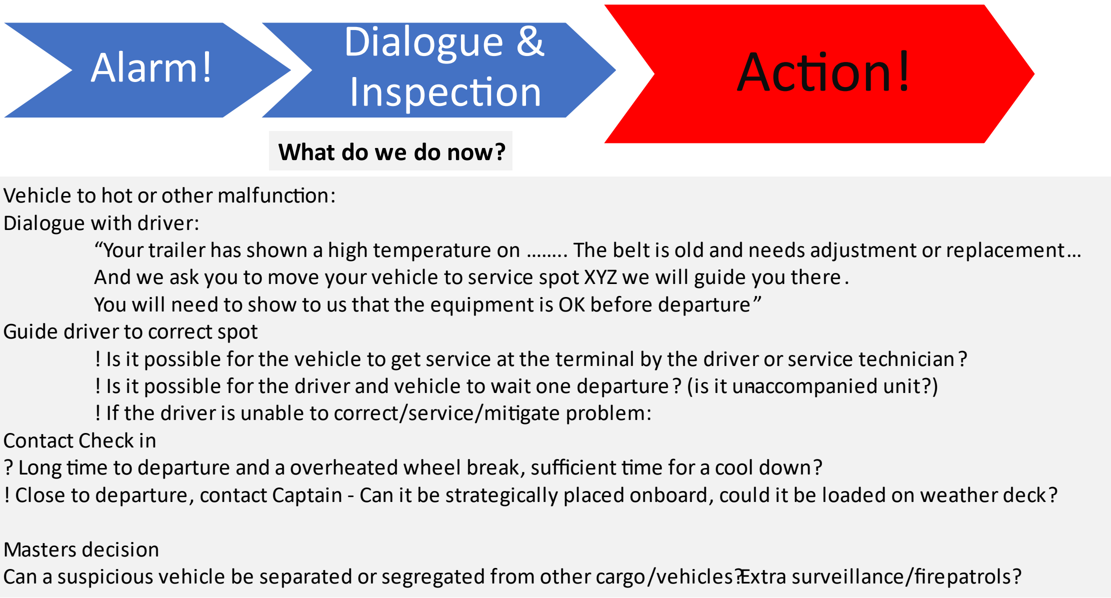

Figure 28 What action should be taken?

Depending on the situation at the terminal is at the moment, what the initial discussion with the driver reveals and if an inspection could be performed. Further actions could be required e.g. cool down, re-run through the VHD for a second opinion, or the vehicle can proceed and be loaded with extra percussion such as stowed at weather deck.
The answer to these and many more questions will vary between companies, terminals, operators and the captain's decision regarding the safety onboard his ship.

A VHD system will require new procedures for both the organization at the terminals as well as onboard the ship. These procedures will update the companies Safety Management Code.

5 AGV hotspot detection prototype

Main author of the chapter: Martin Torstensson, RISE

5.1 General description of prototype

The AGV is fitted with a micro thermal camera module from FLIR, model Lepton 3.5 [7], which has been mounted on a PureThermal-2 FLIR Lepton smart I/O module from GroupGets. The final dimensions of this setup are 30 x 22 x 8 mm, and it is mounted on the front of the AGV with an upward angle. The main purpose of the sensor is to detect temperature anomalies while moving under a parked EV, as EV manufacturers place their battery banks in the area between the wheels under the vehicle. Charging EVs carries the risk of batteries overheating and exploding, which represents an unwanted hazard.

5.2 Camera coverage

For the thermal camera to achieve the purpose of scanning the underside of vehicles or cargo for irregular heat signatures it is paramount that it achieves a sufficient coverage, i.e., the parts of interest in the cargo needs to be within the thermal camera's frame at a distance where it is able to read the values with precision. One of the primary factors to determine the footprint is the height of vehicle or cargo from the ground as it will increase the distance between the drone and the underside. The ground clearance or ride height of vehicles varies depending on the type. Between different vehicles the ground clearance can significantly differ. To give a few examples, a Porsche 911 GT3RS has a height from the ground of 88mm, compared to 14 cm of a Tesla model 3. The Rivian R1T or a R1S are significantly higher at 37.8 cm. This variation can make it challenging to find a setup for the thermal camera that achieves the best coverage. In extreme cases the drone may not even be able to enter underneath a vehicle. This has been a major point of interest during the design as keeping the height of the drone low affects its ability to both scan underneath the vehicles and to move underneath them at all. There are, however, limits to how low it can be designed while still containing all the necessary components to operate. For the calculations and visualizations in this report an assumption of vehicle ground clearance has been set at 15 cm, as it is a realistic value for most current EVs, and the drone cannot reasonably be expected to function far below this ground clearance unless significant changes are made to its design.

A part of the benefits with the 3D model of the drone described in D08.11 is the ability to approximate the thermal camera's footprint while moving under a vehicle. While it is not a perfect representation of reality it creates an environment where it is easier to make modifications while examining their effects on the system. As illustrated in Figure 29 the field of view from the specifications of the thermal camera can been extrapolated out from the model. In the specification of the FLIR Lepton 3.5 [2], the angular field of view (FOV) is specified as 71° and 57° in diagonal and horizontal respectively. These measurements have been used in the model together with a flat plate meant to showcase the undercarriage of a vehicle with the aforementioned ground clearance of 15 cm and a width of 1.6 m. This setup makes it possible to visualize the footprint and estimate how well the coverage will be for different vehicle heights, in addition to choosing an appropriate angle for the thermal camera. As can be seen from Figure 29 one camera is able to fully cover the undercarriage at a distance of roughly 1.5 m, which close enough to achieve acceptable resolution. An angle of 20 degrees from the vertical plane, as seen in Figure 29, was deemed appropriate for the thermal camera based on a visual inspection of the alternatives in the 3D model.

From the experiment visualized in Figure 29 the camera footprint is shown. Note, the camera footprint is not the FOV, as FOV is the size of the image on a flat plane perpendicular to the lens at a given distance. Also, due to the tilted image plane (i.e., not being perpendicular to the optical axis) and a $f_{\#}$ = 1.1 (according to specs. of the thermal sensor) out-of-focus artifacts will be present. However, Scheimpflug adjustments are beyond the scope of the current prototype.

The 3D modelling results showed that the usage of one FLIR Lepton thermal camera was a promising choice if it was placed at a correct angle. The height of the vehicle or cargo does still present a major factor of how large the coverage of the camera is. However, even at relatively low ground clearances, such as 15 cm, the drone can be able to cover the whole width of the vehicle at a distance of approximately 1.5 m. This measurement does not take into consideration cases when the undercarriage is not perfectly flat, but it provides a good indication that the sensor will be sufficient for the task.

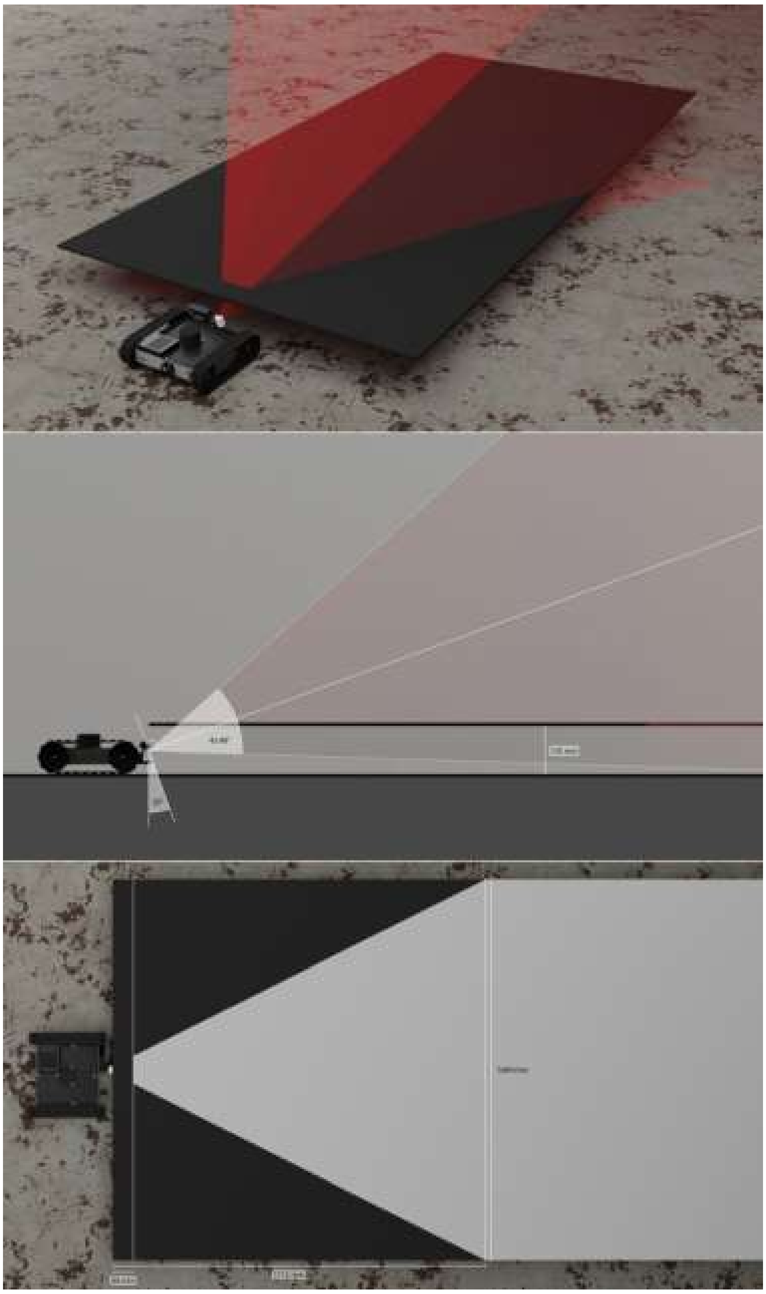

Figure 29. Coverage of a typical passenger vehicle's battery with the IR camera. Top: AGV approaches vehicle with a battery of 1.60m width and 15cm ground clearance. The red cone depicts the field of view (FOV) of the IR camera and how it intersects with the battery. Middle: The thermal sensor is mounted with a fixed angle of 20° on the AGV. It has a horizontal FOV of 57.1°, and a vertical FOV of 43.48°. Bottom: The intersection of the FOV cone with the battery shown in light gray. The full width of the battery is visible in the IR camera's frame at 157.2cm distance.

5.3 Temperature readings in lab environment

Based on the thermal camera, images with temperature readings for each pixel are created. With the task of finding heat anomalies in mind the main goal is to quickly extract information that indicates whether there are any unusual heat signatures that need to be examined more closely. It is mainly cases where the heat anomaly is excessively high that warrant suspicion, as it stands to reason that it is unlikely that a fire may occur due to excessive coldness. To create a system where the most important information can be easily transferred there are two values extracted from the heatmap, namely the highest and the lowest. While it is self-evident that the highest value can be of interest to know the lowest value is also sent as a sanity check and reference. Based on the specifications of the FLIR Lepton 3.5 there is an uncertainty in the temperature that can vary by up to 5 degrees Celsius in either direction. This uncertainty is, however, low in comparison to the temperature differences between an ignition hazard and the ambient temperature that would warrant an alarm by the system.

With the Lepton camera mounted to the drone via a USB connection a test was performed to verify that the installation functions correctly and all the programs are running on the Nvidia Jetson board. The main purpose was to see whether it was functioning correctly in accord with the supplier's specifications. A spot source of heat was placed in front of the thermal camera, and is clearly visible in Figure 30 where it is detected to have a temperature of 73 C compared to the ambient temperature in the room of 19.9 C.

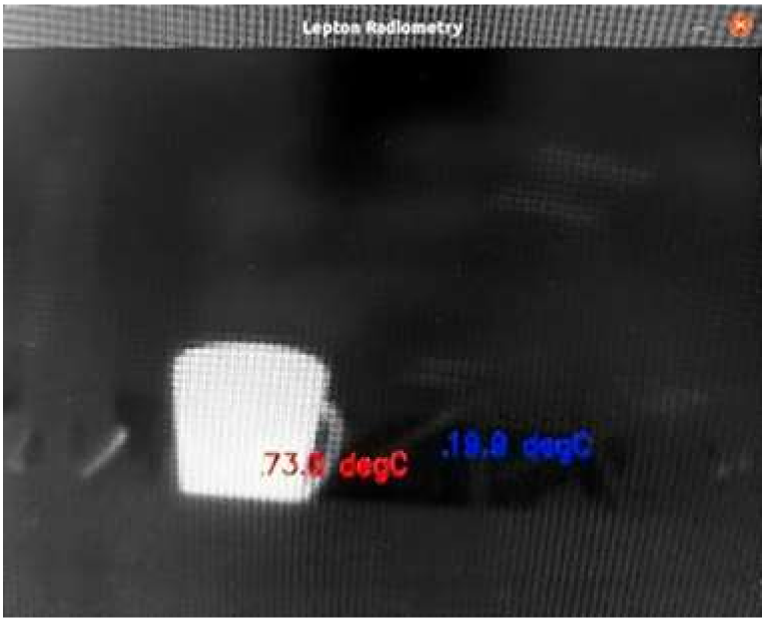

Figure 30. An example of the thermal sensor and its min and max temperature readouts. Here a cup filled with hot water is detected as 73 °C and a background object as 19.9 °C, representing the ambient temperature of the environment.

6 AGV navigation prototype

Main author of the chapter: Leon Sütfeld, RISE

6.1 General description of prototype

The AGV prototype performs navigation and locomotion, i.e., automated driving based on a list of target waypoints. It senses its environment using a 2D LiDAR scanner that detects nearby obstacles in a range of up to 16 meters away. Based on the LiDAR scanner's output, a map of the environment is created and the AGV's position in it is tracked. A pathfinding algorithm then uses this map to generate a path to the next waypoint, and a motor control system drives the two motors of the AGV such that the vehicle follows the path. Once a waypoint is reached, the next waypoint is selected, until there are no more waypoints in the list.

More technically, the AGV prototype uses a sense-plan-act control architecture for automated navigation and locomotion (see figure below). The signal flow for these functions is largely described as a serial succession of individual modules that begins with the 2D-LiDAR system sampling the environment in a 2D plane and ends with each motor receiving a control signal in the form of an 8-bit signed integer (i.e., a number between –127 and 127).

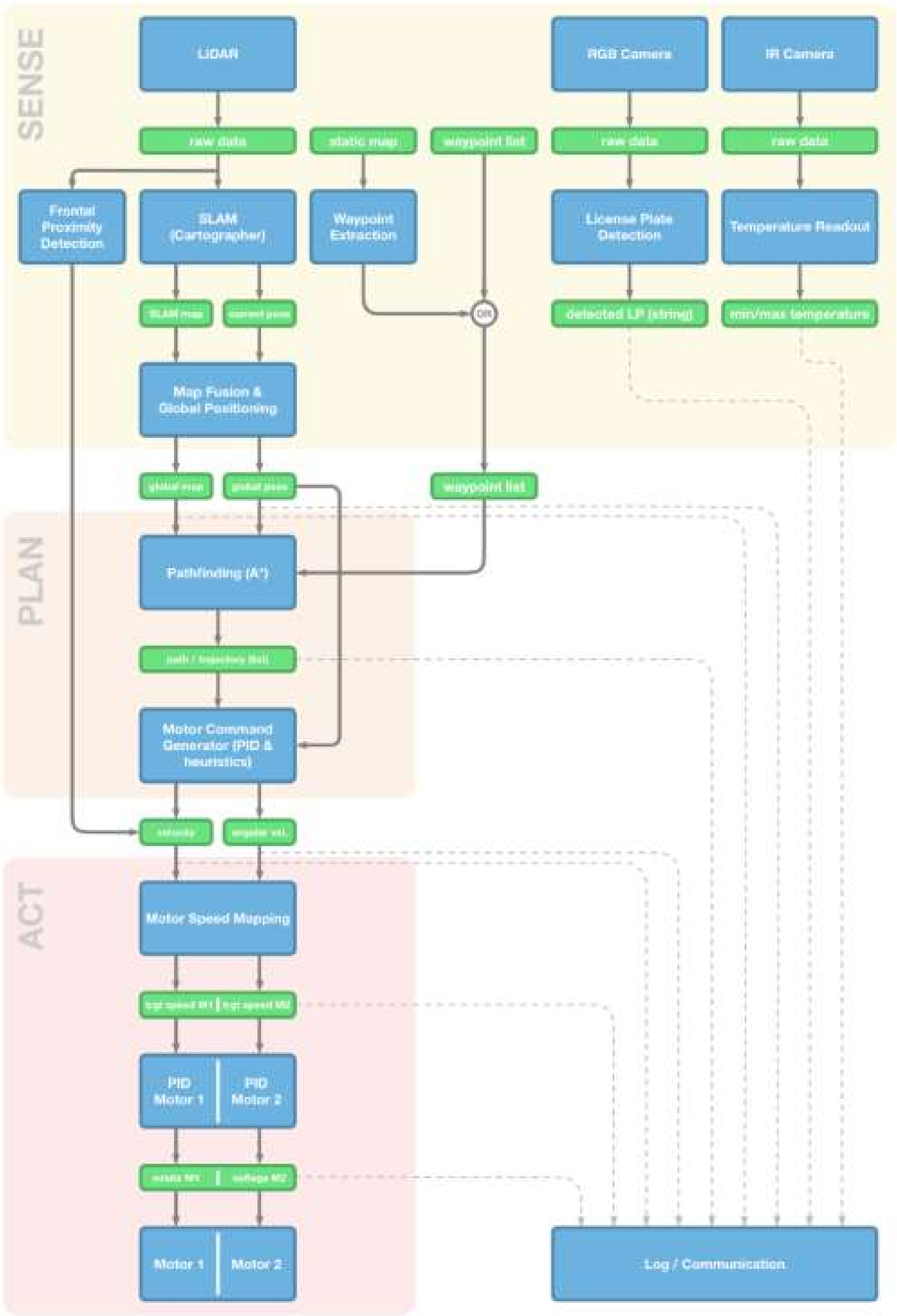

Figure 31. Conceptual sketch of processing flow (sense-plan-act control architecture in the left half, license plate detection and thermal imaging in the top right corner)

While a more detailed description can be found in document D08.11, we shall briefly describe the modules here.

The raw LiDAR data is used by the Simultaneous Localization and Mapping (SLAM) system to create a stable map of the environment, i.e., walls and any obstacles intersecting the 2D plane in which the LiDAR operates, as well as tracking the AGV's location within this environment.

The SLAM data is then combined with a pre-existing static map of the environment (e.g., representing the empty deck of a ferry), which requires thresholding of the map as well as a series of processing steps that rotate the SLAM map and the AGV's position within that map to match the coordinate system of the static environment map. We refer to the joint map as the global map and the AGV's position and orientation within it as its global pose.

A pathfinding algorithm then generates a path to the next of any number of pre-defined waypoints that are to be visited in order. This is followed by a command generator calculating appropriate (target) values for forward velocity and angular velocity based on the calculated path and the AGV'S position and orientation.

Next, the targeted forward and angular velocity values are translated into target speeds for the two individual motors (the AGV is a track-based vehicle and thus steering commands are realized by differential speeds between the left and right tracks).

Finally, the target motor speeds are fed into two individual PID controllers which produce the final control signal for the motors -- the afore-mentioned 8-bit signed integer -- which is then sent to the motors. This loop is repeated indefinitely until the last waypoint is reached.

6.2 AGV demonstration

6.2.1 Test design

The control architecture of the automated driving functions (see Figure 31 above) and the predominantly serial nature of the signal flow within it create a chain of dependencies between earlier and later modules. Later modules typically require all earlier modules to be functional and/or their output to be sufficiently accurate. In many cases, test documentation for modules later in the chain simultaneously document the functioning of earlier modules.

We created a list of isolated functional requirements for all major functional elements of the architecture and document the meeting of these requirements in either specific isolated tests or in combined / full system tests.

6.2.2 Scenario description

In the following, we list the functional requirements for the AGV and the corresponding test scenarios to verify that the requirements are met.

Functional requirements:

R#	Functional element	Requirement	Test
8.1	localization & mapping	static environment map is loaded correctly	T3.1
8.2	localization & mapping	dynamic environment map (via SLAM) is created and sufficiently accurate	T3.1

8.3	localization & mapping	scaling of static map and dynamic map match with sufficient accuracy	T3.1
8.4	localization & mapping	offset-correction between static map and dynamic map is sufficiently accurate	T3.1
8.5	localization & mapping	static and dynamic maps are merged correctly into global map	T3.1
8.6	localization & mapping	AGV location tracking on global map is sufficiently accurate	T3.1
9.1	motor commands	individual motor control via python control command functional	T1.1
9.2	motor commands	motors reach and hold constant a requested motor speed	T1.1
9.3	motor commands	AGV movements reflect requested forward velocity and angular velocity with sufficient accuracy	T2.2/ T3.1
10.1	navigation	waypoint list is correctly read from text file	T3.1
10.2	navigation	waypoint list is correctly created from markers on static map	T2.2
10.3	navigation	pathfinding algorithm finds path from current position to target waypoint	T2.2/ T3.1
10.4	navigation	planned path is followed by appropriate forward and angular velocity commands	T2.2/ T3.1
10.5	navigation	collision avoidance: AGV stops when encountering dynamic obstacle in front of it	T2.1/ T2.2
11.1	system	vehicle navigation functional in relevant real-world scenario (isolated)	T3.1
11.2	system	temperature and license plate readout functional in relevant real-world scenario (isolated)	T3.2
11.3	system	vehicle navigation, temperature and license plate readout functional in relevant real-world scenario (combined)	T3.3
13.1	battery	battery life sufficient for targeted scenario	T4.1

Test scenarios:

T#	Test Scenario	Description
1.1	PID motor control isolated	Target motor speeds are defined and scheduled, and sent to the PID controllers, which create command signals to the motors. The motor speeds are then read out and compared to the requested speeds over time.
2.1	Collision avoidance for dynamic obstacles (lab test)	The AGV is tasked with reaching a waypoint on the map. While it moves towards the target, an obstacle is held in its path, and the AGV is expected to stop before a collision with the obstacle occurs.
2.2	Navigation in lab environment	A parcours with a series of waypoints is defined in a lab or office environment. The AGV is tasked with visiting all reachable defined waypoints while avoiding any obstacle collisions.
3.1	Navigation in relevant environment	A parking garage with parked vehicles is used as an approximation of the conditions found on a ferry's parking deck. Two cars are placed behind each other and the AGV is tasked with passing underneath the vehicles in a straight line, turning around, and returning to a location near the starting point next to the vehicles.

3.2	Temperature readout and license plate detection in relevant environment	In the same parking garage setting, the AGV is placed behind the parked vehicles and tasked with reporting minimum and maximum temperatures in its field of view, as well as reporting the license plate of the vehicle ahead.
3.3	Combined navigation, temperature readout, and license plate detection in relevant environment	This task is a combination of T3.1 and 3.2.
4.1	Battery runtime test	This test consists of the AGV continuously navigating/circling between a set number of waypoints from a full battery charge until depletion to determine the maximum run time of the battery under operating conditions.

6.3 Results

6.3.1 T1.1 - PID motor control isolated

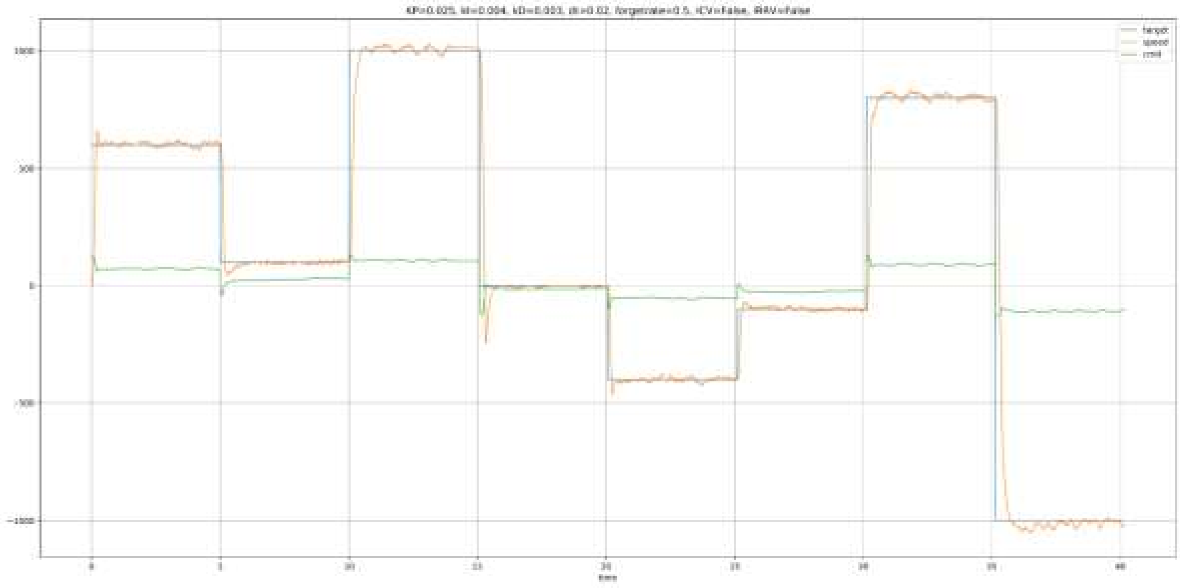

Figure 32. PID based motor control test, stepped. Blue: target speed, orange: achieved speed, green: command signal.

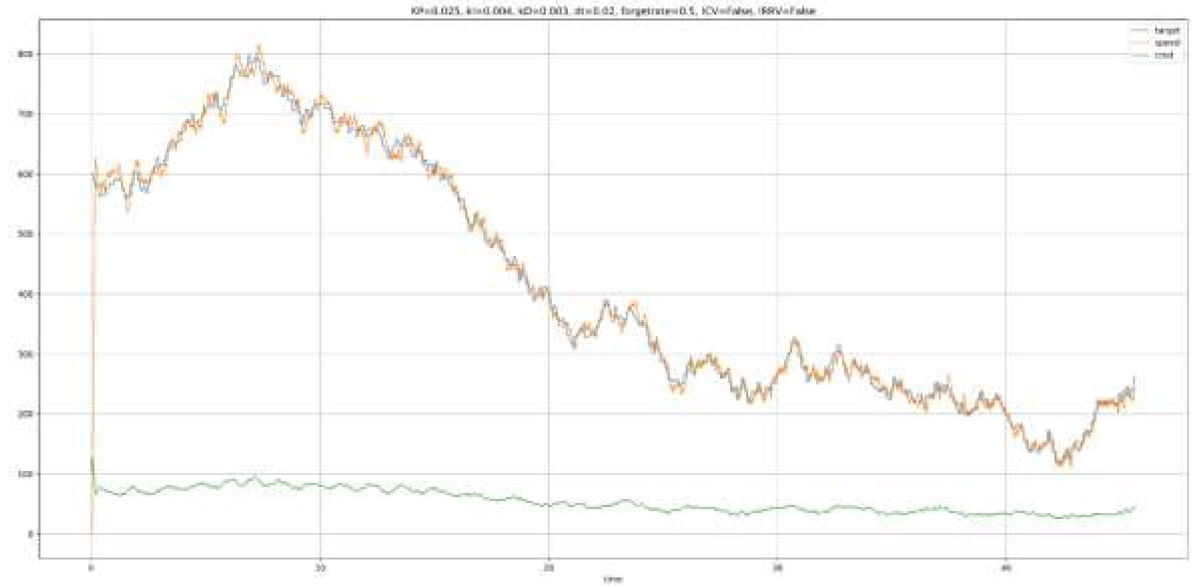

Figure 33. PID based motor control test, random. Blue: target speed, orange: achieved speed, green: command signal.

For the PID motor control test, the AGV's chassis was placed on a box to keep it stationary while the tracks spun freely. This setup is a simplification of the use case scenario but was chosen for the reproducibility of results through any number of runs. Figure 32 and Figure 33 show the test outcomes; target motor speeds (blue) were sent to the PID controller, which produces a command signal (green) such that the requested speed is enacted as precisely as possible. The measured encoder speeds (orange) follow the target closely with minimal errors in both tests, and constant speed targets are met with a near perfectly constant motor output. Thus, requirements R9.1 and R9.2 are fulfilled.

6.3.2 T2.1 - Collision avoidance for dynamic obstacles (lab test)

In this test the AGV was tasked with reaching a target point. On its way towards the target point, an experimenter randomly held an obstacle (license plate) into the AGV's path, to trigger an emergency stopping. While no formal documentation was kept, the AGV stopped immediately once the object was held in front of it and continued moving towards the target point within 1-3 seconds after the object was removed from its path. The test was repeated multiple times with virtually identical results and without any obstacle collisions. Requirement R10.5 is thus met.

6.3.3 T2.2 - Navigation in lab environment

This test consists of the AGV navigating a short parcours in a lab setting (office), including the navigation around a static obstacle between two waypoints. The waypoints were provided via markers in the map file, the test thus covers requirement R10.2. All other elements of this test are also present in T3.1, where a more detailed analysis was carried out. We therefore limit the documentation of this test to the corresponding [video recording]. The successful passing of this test demonstrates that requirements R9.3, R10.2, R10.3, R10.4, R10.5 are met.

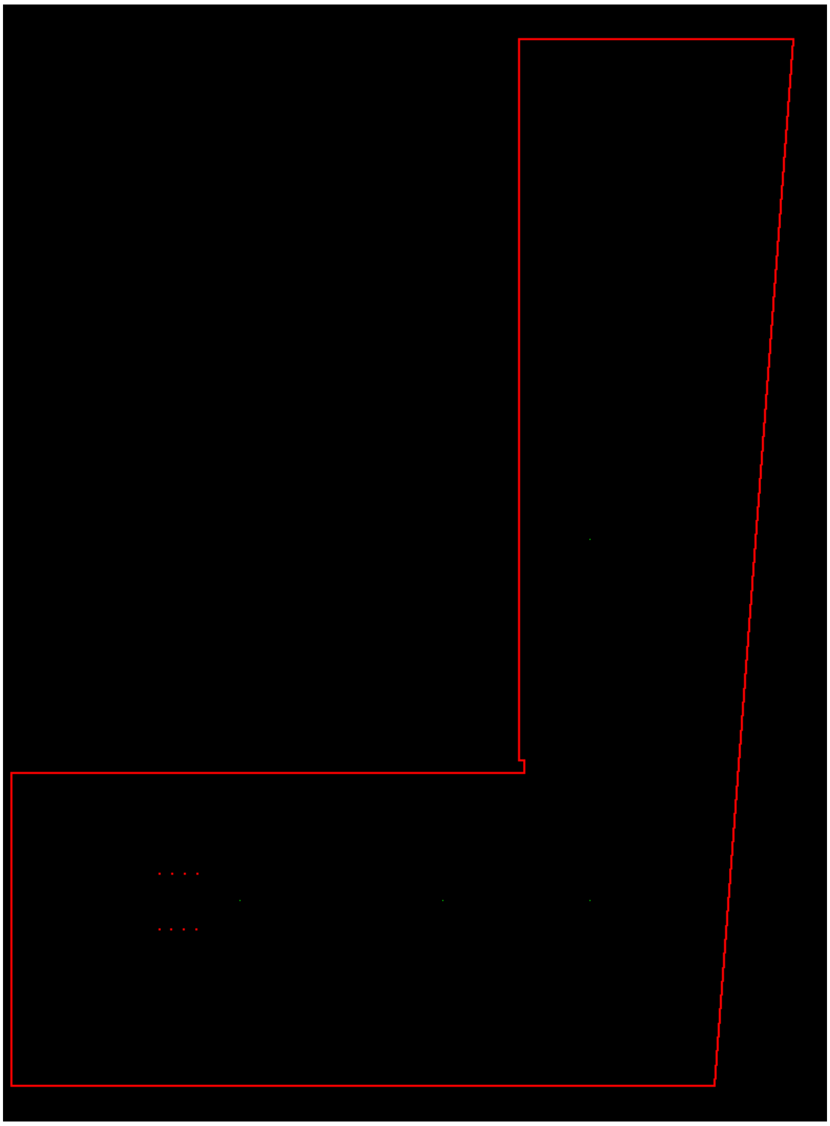

Figure 34. The static environment map used for T.2.2. Red: Solid walls and calibration rig. Green: Waypoints for map-based waypoint parsing.

6.3.4 T3.1 - Navigation in relevant environment

The environment most similar to a ferry's park deck that was accessible and practical for testing was the parking garage at Lindholmen, Gothenburg. A small section of the garage was used as the test site, with two passenger EVs parked in a row. The calibration rig, i.e., the starting position for the AGV (see D08.11 for details), was placed and fixated behind the parked vehicles. A map of the used section in the parking garage had been prepared, and a list of waypoints was created that would guide the AGV to pass under both vehicles before turning around and returning alongside the vehicles to a place near the starting point. Beyond text-based logs, we saved the unprocessed SLAM maps as well as the global maps overlaid with visual markers documenting waypoints, planned paths, the AGV's past trajectory, etc.

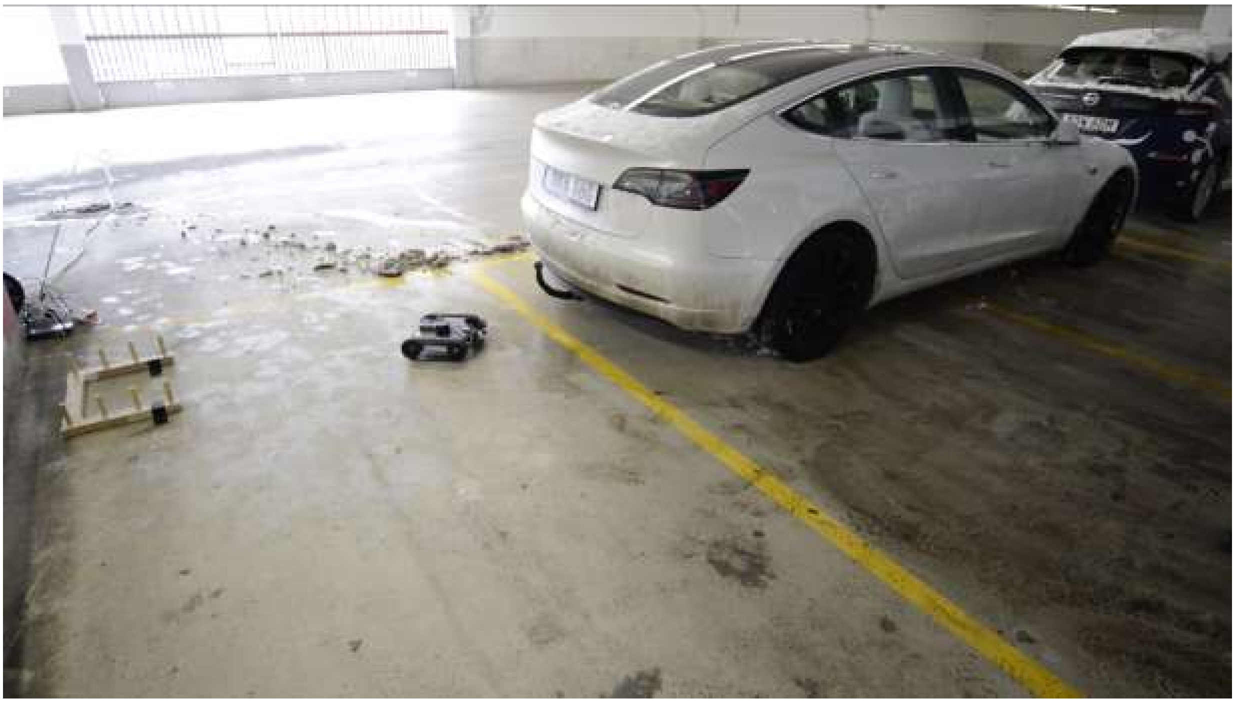

Figure 35. Test setup for tests T3.1, T3.2, and T3.3.

A [video] was created showing synchronized footage from two cameras and the progression of global maps (obstacle detection, tracking, path finding) for this test. The clip demonstrates the AGV's general ability to perform automated driving functions in a realistic environment, meeting requirement R11.1. We will now elaborate further on the meeting of module-level requirements linked to test T3.1.

Figure 36. The static environment map used for T3.1 and T3.3. It is void of waypoint markers, as these were provided via code files.

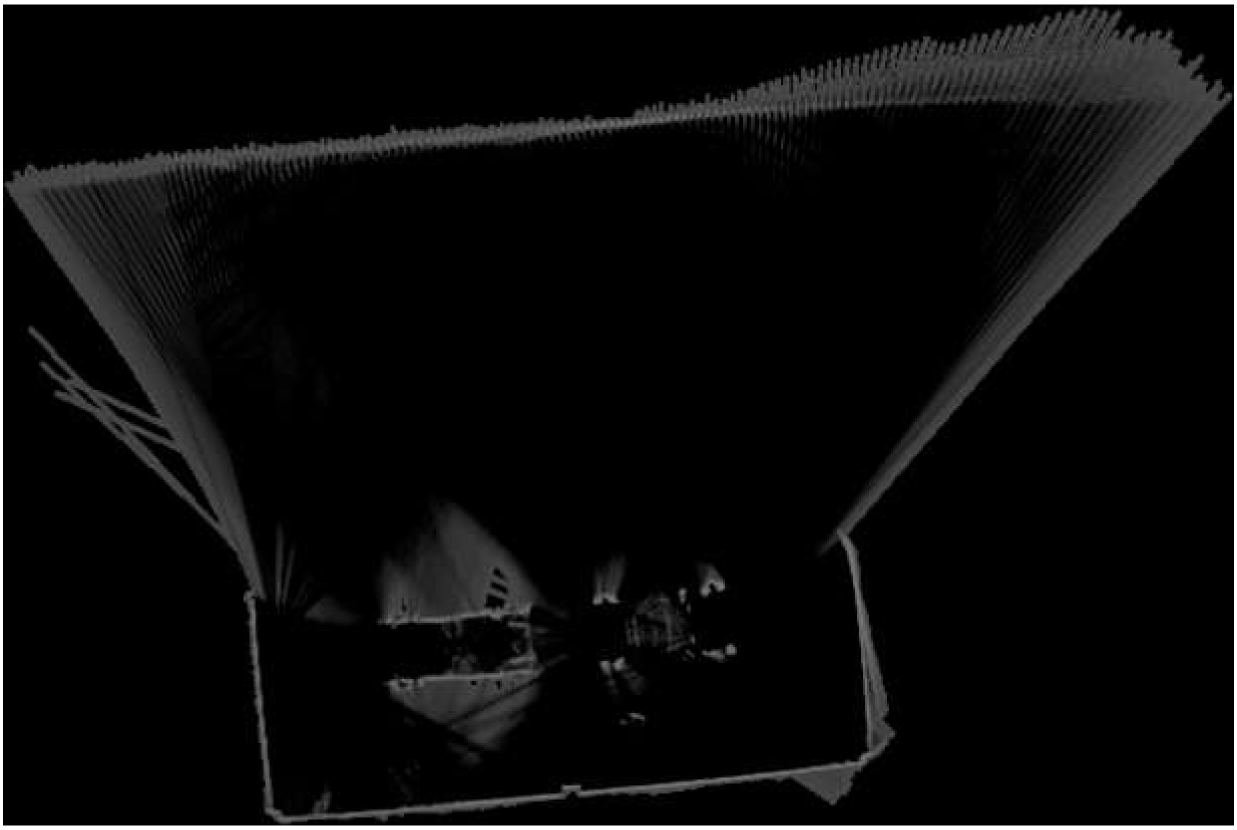

Figure 37. Unprocessed SLAM map after around 50% of the run completed.

Figure 38. Rotation aligned overlay of SLAM map (blue) and corresponding static environment map (brown). Alignment was carried out with the use of the (combined) global map.

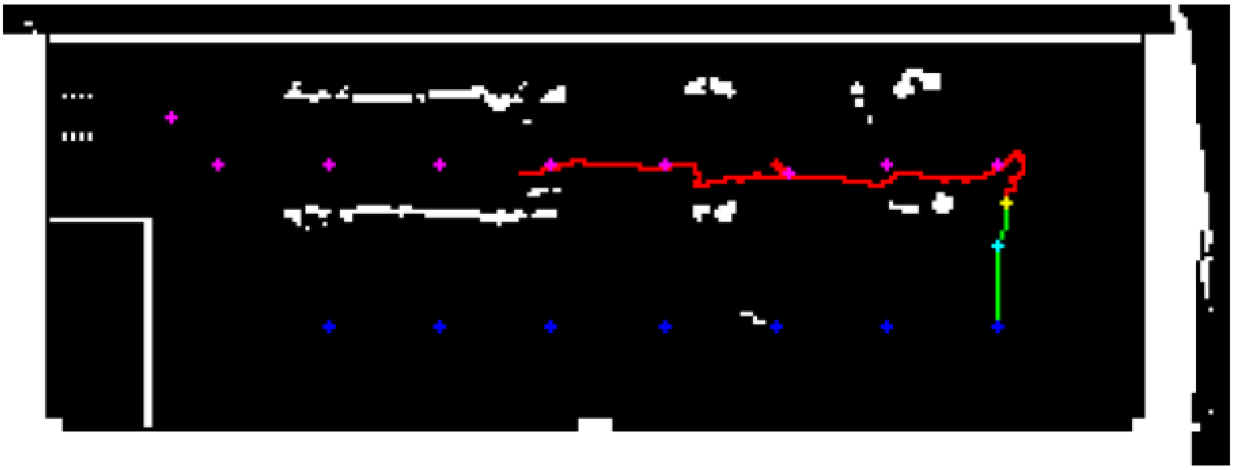

Figure 39. The global map saved by the AGV after around 50% of the run completed. For reasons of computational demand, it is downscaled in resolution by a factor of 5 compared to the static and SLAM maps and therefore more pixelated. White: Solid obstacles, either detected by the AGV's SLAM system or provided in the static environment map. Yellow: The AGV's current position. Red: The AGV's most recent trajectory. Green: The currently planned path. Turquoise: The current target waypoint. Blue: Future waypoints. Pink: Past (reached) waypoints: Red cross-markers: Skipped waypoints (these were unreachable due to obstacle proximity and were therefore progressively shifted to the nearest reachable location).

Figure 36 shows the static environment map used for tests T3.1 and T3.3. Note that additional "imaginary" walls were placed in the map to prevent the AGV from leaving the defined area at the top, or entering the area designated for test-equipment and engineers (lower left).

Figure 37 shows the unprocessed SLAM map after completing around 50% of the run. Defined outlines for the surrounding walls are visible, as are the two vehicles. However, both vehicles show accumulated evidence for the existence of obstacles in places other than the wheels. This issue occurs solely but reliably in vertically confined spaces and is related to the LiDAR's slightly upward tilt angle; the [YDLIDAR G4 specification] indicates 0.25° to 1.75°. Per meter distance from the LiDAR, a 1.75° upwards tilt angle would result in a 3.1cm upward shift for the laser beam, leading to the potential detection of overhead obstacles for all distances greater than about one meter away from the LiDAR. We therefore consider requirement R8.2, the creation of a sufficiently accurate SLAM map, to be only marginally met and discuss this issue further in D08.11.

Figure 38 is a manually created overlay of the unprocessed SLAM map (Figure 37) and the static environment map (Figure 36). The basis for the manual matching of the two maps was the global map saved by the AGV during the run; it is therefore an accurate recreation of the map-matching happening in the map fusion module.

The overlay shows the scaling between the two maps to be sufficiently close (R8.3 met), although slight improvements could still be made. Aside from a minor mismatch in scaling, the two maps are very precisely matched (R8.4 met): The rotation is closely matched, as evident from the alignment of the bottom wall, and the translational offset around the location of the calibration rig (top left) appears to be minimal. The correct merging of static and SLAM maps (R8.5) is, therefore, also met.

We further consider requirement R8.6 (AGV tracking accuracy within the map) to be met, as the SLAM maps created via inside-out map building are limited in accuracy by the tracking accuracy of the AGV. In other words, if the AGV's tracking on the map were inaccurate, the created maps would be too. Since they are very precise aside from their scaling, the AGV's position within them is too. Thusly, the [video] also shows the AGV's tracked trajectory to match the real-world trajectory very well.

The global map, shown in Figure 39, is the outcome of the map fusion module on the AGV; an on-the-fly combination of static map and SLAM map -- thresholded, downscaled, and enhanced with relevant markers. The successful loading of the static map (R8.1) follows from its inclusion in the global map, as does the successful loading of waypoints from a list (R10.1).

Requirement R10.3 demands that an appropriate path to the next waypoint is found. This is the case, as can be seen in Figure 39 as well as the [video]. Note that to achieve smoother operation, the path from any current waypoint A to the following waypoint B is also already computed as soon as the AGV is within a defined distance from A. Note also that the "phantom obstacles", detected due to the upward tilt angle of the LiDAR system, occasionally block the straight-line path between the AGV and the next waypoint. As intended in those cases, the path planning algorithm creates a path around the detected obstacles.

Finally, the meeting of requirements R9.3 and R10.4 -- the creation of appropriate forward velocity and angular velocity commands, as well as their sufficiently accurate enactment – follows from the successful reaching of all waypoints. However, additional fine tuning of parameters in the forward and angular velocity command generation might yield smoother operation of the drone.

6.3.5 T3.2 - Temperature readout and license plate detection in relevant environment

This test was conducted in the same environment as T3.1, with the drone statically placed behind the vehicles and inside the calibration rig (see Figure 40). The readout and logging procedure for temperatures and license plates were activated. The log file outputs show repeated readouts such as the following:

```
minTemp = -3.85 C
maxTemp = 7.97 C
detection: RKW36G
```

While we did not have any way of formally confirming the temperature readouts, they are highly plausible given ambient temperatures of around -4°C (according to The Weather Channel) at the time of testing. The license plate readout was found to be functional albeit somewhat inconsistent; in a significant fraction of repeated reads, it was recognized as "RKW6G", thus missing the "3", despite the favourable viewing angle and occlusion-free line of sight. We thus consider requirement R11.2 as partially met.

Figure 40. Setup for isolated readouts of temperatures and license plate (T3.2).

6.3.6 T3.3 - Combined navigation, temperature readout, and license plate detection in relevant environment

This test consisted of the combination of T3.1 and T3.2, i.e., the simultaneous running of the automated driving functions, and license plate and temperature readouts, and was carried out in the same environment as T3.1 and T3.2.

Unfortunately, the AGV's behaviour was found to be inadequate and partially erratic. The reason for this behaviour was determined to be exceedingly long compute times for individual modules in the automated driving functions, which may have been caused by the simultaneous running of automated driving functions and license plate detection, and their competition for compute resources. Significantly extended compute times lead to a desynchronization between the tracking and pathfinding and the real-world position and orientation of the AGV, resulting in generated commands that no longer fit its current pose. Requirement R3.3 was thus failed, and approaches to overcome this issue are discussed in document D08.11.

6.3.7 T4.1 - Battery runtime test

This test was planned to have the AGV perform a continuous driving task in an endless loop until the batteries are depleted. However, the chosen LiPo batteries proved highly susceptible to low charging states, i.e., once a certain low voltage level is reached, they lose their ability to be recharged and are effectively dead. This happened numerous times during the development process of the AGV, and the planned test would have most likely resulted in another lost battery. Instead, we opted for a theoretical assessment of the battery time, focused on the battery powering the main compute device and connected sensors, as it was found to be the quicker to deplete battery.

The Nvidia Jetson AGX Xavier ran in a 15W mode for the APU, and an estimated board draw of ca. 20W (due to chipset, ram, I/O controllers, and power converters). We estimate the connected sensors and WiFi antenna to consume another 10W, resulting in an estimated system power draw of around 30W. The batteries used were rated at 5200 mAh for the voltage range from 12.6V to 9V. However, without a battery management system (BMS) in place the individual cells are not depleted at the same rate, and we had to limit the used voltage range to a minimum of about 10.8V to avoid damage to the batteries. This leaves only 2600 mAh, or 29 Wh at 11.1V, the theoretical estimate of battery run time is thus 58 minutes. With that, we count the requirement R13.1 as technically fulfilled. However, as discussed in document D08.11, a switch to a different battery type, such as lithium ion, together with a BMS would be highly desirable for real world use of the AGV.

7 Conclusion

Main author of the chapter: Martin Torstensson, RISE

A demonstrator for a VHD system located at Majnabben in Gothenburg has been shown describing and visualizing its functionalities. The systems’ capabilities of detecting heat and measuring the length and of the vehicles passing through the system have been tested. Machine learning for segmentation of the top side of the vehicles making it possible to locate the refrigeration AC unit in the void between truck and trailer has been tested successfully. A base line for normal temperatures measured on operating refrigeration AC units has been concluded and tested with the capability to raise alarms connected to high temperatures on AC refrigeration units for Majnabbe terminal.

Another demonstrator of the AGV system has also been developed and evaluated. Its abilities to navigate have been demonstrated in a parking garage to simulate a similar environment to a ship and lab tests have also been performed. It shows a good ability to avoid and navigate around objects in a self-sufficient manner without the need of landmarks other than a calibration rig at the origin.

Both the VHD and AGV system have demonstrated the use of license plate reading as a way to connect the vehicle to a higher level of information, it could be a booking system, terminal operation system, stowage planning tool (SPT) or firefighting resource management centre (FRMC).

8 References

[1] Guidance MGN 653 (M) Electric vehicles onboard passenger roll-on/roll-off (ro-ro) ferries Retrieved from: URL https://www.gov.uk/government/publications/mgn-653-m-electric-vehicles-onboard-passenger-roll-onroll-off-ro-ro-ferries [Accessed March 2023]

[2] D08.2 Fire hazard mapping visualization tool with fire hazard matching integrated (January 2022) https://lashfire.eu/media/2022/02/LASH-FIRE_D08.2_Fire-hazard-mapping-visualization-tool-with-fire-hazard-matching-integrated.pdf [Accessed March 2023]

[3] D08.11 Description of prototypes and demonstration for identification of vehicles and ignition sources. https://lashfire.eu/media

[4] EMSA. (2021, 03 12). *Fire safety in ro-ro passenger ships – FIRESAFE studies*. Retrieved from:www.emsa.europa.eu: http://www.emsa.europa.eu/firesafe.html [Accessed March 2023]

[5] In-door positioning on RoRo vessels, RISE Viktoria https://lighthouse.nu/images/pdf/indoor_positioning_webbcompressed-1.pdf [Accessed March 2023]

[6] LASH FIRE. (2020). *LASH FIRE Deliverable D04.1* Review of accident causes and hazard identification report: https://lashfire.eu/media/2021/04/LASH-FIRE_D04.1_Review-of-accident-causes-and-hazard-identification-workshop-report.pdf [Accessed March 2023]

[7] FLIR. (2021). FLIR. https://www.flir.eu/products/lepton/ [Accessed: 2023-03-17]

9 Indexes

9.1 Index of tables

9.2 Index of figures